END

FILMED

MICROCOPY RESOLUTION TEST CHART
NATIONAL BUREAU OF STANDARDS-1963-A

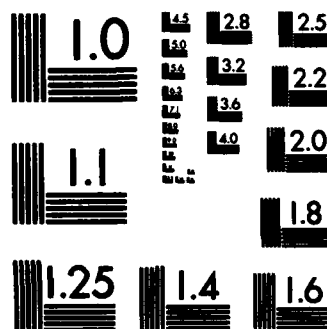| REPORT DOCUMENTATION PAGE		READ INSTRUCTIONS BEFORE COMPLETING FORM
1. REPORT NUMBER Technical Report No. 15	2. GOVT ACCESSION NO. AD-A134 031	3. RECIPIENT'S CATALOG NUMBER
4. TITLE (and Subtitle) Arrays of Very Small Voltammetric Electrodes Based on Reticulated Vitreous Carbon		5. TYPE OF REPORT & PERIOD COVERED
		6. PERFORMING ORG. REPORT NUMBER
7. AUTHOR(s) Neal Sleszynski, Janet Osteryoung and Malcolm Carter		8. CONTRACT OR GRANT NUMBER(s) N00014-79-C-0682
9. PERFORMING ORGANIZATION NAME AND ADDRESS Department of Chemistry/Department of Dental Materials State Univ. of New York at Buffalo		10. PROGRAM ELEMENT, PROJECT, TASK AREA & WORK UNIT NUMBERS NR-056-715
11. CONTROLLING OFFICE NAME AND ADDRESS Office of Naval Research/Chemistry Program Arlington, Virginia 22217		12. REPORT DATE October 14, 1983
		13. NUMBER OF PAGES 37
14. MONITORING AGENCY NAME & ADDRESS(if different from Controlling Office)		15. SECURITY CLASS. (of this report) Unclassified
		15a. DECLASSIFICATION/DOWNGRADING SCHEDULE

16. DISTRIBUTION STATEMENT (of this Report)

Approved for Public Release: Distribution Unlimited

17. DISTRIBUTION STATEMENT (of the abstract entered in Block 20, if different from Report)

18. SUPPLEMENTARY NOTES

Prepared for publication in _Analytical Chemistry_.

19. KEY WORDS (Continue on reverse side if necessary and identify by block number)

Reticulated vitreous carbon; microelectrodes; nonlinear diffusion; voltammetry

20. ABSTRACT (Continue on reverse side if necessary and identify by block number)

Micro-electrode arrays constructed from reticulated vitreous carbon are described and characterized. Sterological analysis and cyclic voltammetric data indicate the arrays have equivalent radii as small as 32 microns, with densities as high as 1650 electrodes/cm^2.

83 10 24 032

DD FORM 1473 EDITION OF 1 NOV 65 IS OBSOLETE
1 JAN 73

DTIC ELECTE
OCT 25 1983
S D
D

DTIC FILE COPY

AD-A134031

Accession For

NTIS GRA&I	X
DTIC TAB	[]
Unannounced	[]
Justification	

By____
Distribution/

Availability Codes

| Dist | Avail and/or Special |
| A | |

ARRAYS OF VERY SMALL VOLTAMMETRIC ELECTRODES

BASED ON RETICULATED VITREOUS CARBON

by

NEAL SLESZYNSKI AND JANET OSTERYOUNG

DEPARTMENT OF CHEMISTRY

and

MALCOLM CARTER

DEPARTMENT OF DENTAL MATERIALS

State University of New York at Buffalo
Buffalo, New York   14214

October, 1983

BRIEF

Micro-electrode arrays constructed from reticulated vitreous carbon are described and characterized. Sterological analysis and cyclic voltammetric data indicate the arrays have equivalent radii as small as 32 microns, with densities as high as 1650 electrodes/cm^2.

ABSTRACT

Arrays of very small electrodes were constructed from nonconductive epoxy and reticulated vitreous carbon (RVC), polished to give a smooth two dimensional surface. The resulting electrodes yield nearly steady state currents at convenient rates of potential scan. Comparison of current densities with those at a normal glassy carbon electrode indicates that on the time scale of seconds non-linear diffusion is the predominant mode of mass transport to the electrode surface. The approach to steady state current is related to the ratio of boundary length to surface area for the various arrays. Equivalent radii calculated from the boundary densities as if the carbon structures on the electrode surface were disks agree well with equivalent radii calculated from experimental data using the ratio of the forward and reverse currents.

The analytical application of very small voltammetric electrodes was first prompted by neurophysiological problems, both in vitro and in vivo (1-3), which required electrodes with small dimensions. Very small potentiometric electrodes have been widely used for physiological measurements for some time (4). Apart for the physical size of very small voltammetric electrodes, they have other advantages arising from non-linear diffusion at conveniently short times which suggest that they should be generally useful in analysis (5). Single electrodes of very small dimensions have, however, the disadvantage of requiring specialized instrumentation for measurements of currents. Therefore, when small overall dimensions are not required for other reasons, arrays of very small electrodes provide the possibility of achieving the desireable characteristics arising from non-linear diffusion together with easily measurable currents. The first arrays of this kind were constructed using photo-resist technology from the semi-conductor industry to form a Clark-type electrode with multiple cathodes for the measurement of pO_2 (6). We have previously used arrays of electrodes based on glassy carbon covered with a polymethylmethacrylate (electron beam resist) insulating layer through which micron-size holes were made to form an active electrode array (7). These electrodes were suitable for testing theories of non-linear diffusion to disks, but not rugged enough for routine analytical use. Recently Wightman et al. have employed arrays of carbon fibers for use as a voltammetric detector in high performance liquid chromatography (HPLC), in which detection is often limited by noise originating from pulsing of the pump (8).

Scharifker and Hills have studied the nucleation of mercury on platinum and carbon micro-electrodes (9). These electrodes have small enough dimensions (8 - 10 μm in diameter) so that only one nucleus is formed on

the electrode surface. This makes it possible to determine the induction period for the formation of individual nuclei at a given over-potential. Mercury films on micro-electrodes have proven analytically useful for anodic stripping voltammetry (ASV). Anderson and co-workers (10) have deposited mercury films on carbon single fiber electrodes with 8 μm radii and determined cadmium by ASV at the ppb and sub-ppb level.

Weisshaar and Tallman (11) have examined the behavior of composite electrodes constructed from Kel-F and graphite. In the range of 5-25% graphite these electrodes exhibit micro-electrode behavior and, when examined by electron microscopy, appear as very small islands of graphite in an insulating plane of Kel-F. They attempted to calculate the equivalent micro-electrode radius of these electrodes from their chronoamperometric behavior using the equation derived by Matsuda and co-workers (12). Only when a bimodal distribution of micro-electrode sizes was assumed was good agreement obtained.

For very small electrodes at sufficiently long times, mass transport, and hence the current, depends only on electrode dimension. For example, for the desirable geometry of the disk embedded in an insulating plane, the limiting steady state current, i_{ss}(μA), is given by the well-known expression

$$i_{ss} = 4nFDC^{o}a \qquad (1)$$

where n is the number of electrons per mole (equiv/mole), F is the value of the Faraday (C/equiv), D is the diffusion coefficient of the reactant (cm^2/s), C^o is its concentration (mM) and a is the electrode radius (cm). The current i_{ss} is proportional to the electrode radius and thus, for the typical case in which backround current is proportional to area, the ratio of faradaic to backround current should increase with decreasing electrode

radius. Furthermore, the steady state diffusion layer thickness, δ_{ss}, is given by

$$\delta_{ss} = nF(\pi a^2)DC^0/i_{ss}$$

$$= \pi a/4 \tag{2}$$

and is approximately the same as the electrode dimension, a. Any process such as convection, with larger characteristic layer thicknesses, will not influence the steady state current. This is the basis for the use of these electrodes in flowing systems, for when the dimension a is small enough the signal should be independent of flow characteristics, in particular the time dependent components of the pumping system (8).

Design of small electrodes to achieve steady state currents requires knowledge of time dependence of the current under conditions of diffusion control (12-15). For our purposes it is sufficient to examine the ratio of the limiting diffusion layer thickness arising from linear diffusion, $\delta_l = \sqrt{\pi D t}$, to δ_{ss} : $\delta_l/\delta_{ss} = 4\sqrt{Dt}/(\sqrt{\pi}a)$. For convenience we consider the dimensionless time $\tau = 16Dt/\pi a^2$. When $\tau \gg 1$, $\delta_{ss} \ll \delta_l$ and steady state currents are attained. For $\tau \ll 1$, $\delta_l \ll \delta_{ss}$ and linear diffusion controls the current. In the intermediate region mixed behavior is observed.

Very small electrodes (i.e., those with $\tau \gg 1$) show effects of slow charge transfer when the steady state diffusion layer thickness (eq. 2) is comparable to the kinetic diffusion layer thickness, $D/k^{0'}$, where $k^{0'}$(cm/s) is the apparent formal heterogeneous charge transfer rate. Swan (16) has derived an equation which describes the influence of kinetics as a function of the electrode radius for spherical diffusion,

$$i = \frac{nFDk^{0'}C^0}{D + 2k^{0'}a} \tag{3}$$

where i ($\mu A/cm^2$) is the exchange current density and the other symbols have their normal meanings. When $D/k^{O'} \gg 2a$, charge transfer is rate determining and $i = nFk^{O'}c^O$. But for $D/k^{O'} \ll 2a$, the reaction is diffusion controlled and $i = nFDC^O/2a$, the steady state current density for spherical diffusion. When $D/2k^{O'}a \sim 1$, the voltammogram will show mixed control.

Arrays of small electrodes connected in parallel behave quantitatively as an equivalent number of individual micro-electrodes when the spacing between them is sufficiently large. At long times the diffusion layers of individual electrodes may overlap, resulting in a decrease in the (formerly) steady state current. The time at which this occurs is a function of both the electrode size and the spacing in the array. Many workers have investigated this problem theoretically (Ref. 15, 27, and references therein). Their results show that at very short times the chronoamperometric current is best described by linear diffusion to the active electrode area. Conversely, at very long times the current is that arising from linear diffusion to the total electrode area, including the insulating spaces between the individual electrodes. In the time regime between these two extremes the current is governed by non-linear diffusion, and the diffusion layers expand across the insulated surface at the rate $\sqrt{\pi D/t}$. Diffusion phenomena of this type are important in studies of charge transfer at partially blocked surfaces.

We have investigated the behavior of a new class of electrode arrays which exhibit the desirable non-linear mass transport properties of micro-electrodes. These arrays are constructed from a composite prepared by filling the voids of reticulated vitreous carbon (RVC) with non-conductive epoxy to produce a two dimensional electrode material. RVC has been widely used for a number of years as a three dimensional,

highly porous electrode material. Although its greatest utility has been for studies in flowing systems (17-19), it has also been used in thin slices as an optically transparent electrode (20) and as a high surface area electrode for coulometry (21). The high void volume and high surface area of RVC translate into large separations between relatively small electrode segments with large perimeters when the RVC is viewed in cross section as a two dimensional structure. This is the first report of its use as a two dimensional electrode. While the individual carbon structures on the surface are rather large, the unusual shape conferred by the cell structure of the RVC produces arrays of electrodes, each active member of which has a large boundary density (boundary per unit area). It is this characteristic which produces non-linear diffusion, and hence approach to steady-state currents at moderate times.

Stereological analysis was used to characterize those geometric aspects of this new class of electrode which could be correlated with the electrochemical properties sensitive to mass transport. The most important are the surface area fraction of carbon, A_a, the boundary density of carbon, P, and the deviation from planarity as determined by interference microscopy.

These arrays show many of the characteristics of the single micro-electrodes and micro-arrays previously studied. They are extremely easy to construct and, unlike the electrodes prepared by photo-resist methods described by Siu and Cobbold (6) and others (13), can be fabricated without special equipment from readily available and inexpensive materials. The estimated material cost of these electrodes is 1-2 dollars per electrode.

EXPERIMENTAL SECTION

Materials: The reticulated vitreous carbon was obtained from Normar Industries, Anaheim, California. The structure is characterized by two numbers, the compression factor, which for this study was limited to 2 x 1 and 4 x 1, and the number of pores per linear inch (45, 60, 80 and 100 were used). In general the higher the compression factor the thicker the carbon fiber produced. The number of pores per linear inch determines the density of the individual electrode surfaces in the final product.

The silver epoxy used for electrical connections was Eccobond Solder 57C manufactured by Emerson and Cuming, Canton, Massachusetts.

The insulating epoxy used in all applications was Buehler epoxide resin and hardener, catalog numbers 20-8130-032 and 20-8132-032. The polisher used to polish the RVC electrodes was a Buehler Minimet automatic polisher and all polishing supplies were obtained from Buehler, Evanston, Illinois.

Electrode Construction: A glass tube, 6 mm i.d., was used as a punch to remove a core of RVC from a block 1 cm thick. The RVC plug was then cleaned with an air jet to remove any loose carbon particles created by the punch. The non-conductive epoxy was mixed as per manufacturer's instructions and poured into acrylic molds (6 mm i.d.) and the RVC plugs lowered into the epoxy so that approximately 2 mm remained above the surface of the epoxy. After the epoxy had set for 8 hours the remaining top 2 mm was filled with conductive epoxy and a small nut attached for future electrical contact. After another 8 hours the unit was removed from the mold and placed in the center of another mold, 10 mm i.d., which was then filled with enough non-conductive epoxy to completely surround the hardened epoxy plug and cover the top surface of the nut. This layer serves to insulate the electrical contact from the test solutions. After the epoxy had hardened, the electrode

was removed from the mold and the surface cut back 2-3 mm with a diamond saw, exposing the two dimensional RVC structure. The surface was then polished using a Buehler Minimet polisher (22) starting with 45 micron diamond and working down in steps to 0.25 micron diamond. The final polishing step was 0.05 micron alumina.

Figure 1 shows a diagram of the finished electrodes. An important feature is that the nut for electrical contact is isolated from the solution by the same epoxy sheath which insulates the rest of the electrode. For convenience the electrode shaft is also made from the same non-conductive epoxy molded around a co-axial cable.

Stereological Analysis: Point and intercept counts were made on the five different types of electrodes (2 x 1 45 and 100, 4 x 1 60, 80 and 100) using a projection microscope and transparent overlay grid (23, 24). Not less than thirty fields were sampled per parameter per specimen by rotating and translating the specimen. This produced sampling precision within approximately 5% (relative standard error of the mean in percent) for all the parameters measured.

Procedure: All experiments were conducted in solutions of 1.0 M KCl, the pH ranging from 2.6 to 7.6. The $K_4Fe(CN)_6$ used was reagent grade and was used without assay or further purification. A commercial SCE with a Vycor frit and a Pt counter electrode were used for all experiments. The electrodes were polished using a Buehler Minimet polisher designed for metallurgical samples as described above. Before each experiment the electrodes were repolished with 0.05 micro alumina and then briefly rinsed with 95% EtOH. Before the addition of the $K_4Fe(CN)_6$ to the buffered solutions the electrodes were cycled between the initial and final potentials (0.0 V and 0.8 V respectively) at 100 mV/s for ten minutes.

The purpose of this cycling was to reduce the backround currents to a lower, constant value. The resulting electrodes had useful potential ranges very near that of normal GCEs, e.g. at pH 2.7 in 1 M KCl the anodic limit is approximately +0.9 V vs. SCE and the cathodic limit is -1.3V. All test solutions were purged with purified argon.

RESULTS AND DISCUSSION

Micrographs of typical finished electrode surfaces are shown in Figure 2.
The electrodes were characterized geometrically by measuring the fraction
of the surface area occupied by carbon (ie, the active surface fraction)
and the boundary lengths. Area fractions, A_a, were calculated for each
field as the number of hits by the overlay grid intersections on the
carbon divided by the total number of test points applied to the microstructure.
Boundary lengths per section were calculated as follows:

$$L_a = (P_{v,h}/L_{v,h})M(\pi/2) \tag{4}$$

where $P_{v,h}$ = # of vertical and horizontal test line intersections

M = magnification

$L_{v,h}$ = total length of the vertical and horizontal lines in the overlay grid

The results of these measurements are summarized in Table I. Means,
standard deviations and standard errors were calculated for the above
ratio estimates by using the statistics developed by Cochran (25).

The actual boundary lengths of the carbon structure were calculated by
multiplying L_a by the area of the total cross section. The boundary density,
P, is the mean boundary length per mean carbon area, or $\bar{L}_a/\bar{A}_a$. Theoretical
values for this ratio for a disc, square and equilateral triangle are 2/a,
4/a, and 6.9/a respectively, where a is either the radius or the length of
a side. For a rectangle, the ratio approaches 2/a as the length of the short
side, a, approaches zero. For shapes with some of the characteristics present
in the carbon micro-structure, such as a square and triangle with concave
sides, the values for this ratio are 7.3/a and 19.5/a respectively.
These models were based on the shapes created between touching circles
of equal radius. Thus, the larger the experimental value of P, the more

complex the shape of the active carbon area. The uncertainty in this parameter, $W_{L,a}$, was derived by a method discussed by Kline and McClintock (26) and is given by:

$$W_{L,a} = [(\frac{\partial B}{\partial A_a} W_{A_a})^2 + (\frac{\partial P}{\partial L_a} W_{L_a})^2]^{1/2} \tag{5}$$

where W_{A_a} = the uncertainty in A_a

and W_{L_a} = the uncertainty in L_a

In this study, 95% confidence limits were used for W_{A_a} and W_{L_a}.

Preliminary topographical analysis was also conducted using interference microscopy. During polishing, composites containing materials with different hardnesses erode nonuniformly. Measurements on these electrodes after polishing showed that the carbon surfaces are higher than the surrounding plane formed by the insulating epoxy. The carbon structure shown in Figure 2b ascends gradually, reaching an elevation at its center approximately 0.5 microns above the surrounding plane of epoxy. Since this is less than 2% of the total width of this particular structure, and the micro-electrode diffusion layer is hemispherical at long times (15), this deviation from planarity should not greatly affect the characteristics of mass transport to the electrode. Materials which have a greater carbon density, such as the 4 x 1 60 and 80 samples, show elevations in excess of 2 microns, which is the useful limit of the interference technique used for these measurements. For purposes of understanding the diffusion phenomena characteristic of these electrodes and ensuring quantitatively reproducible behavior from electrode to electrode, polishing to a flat surface is essential. However, for analytical purposes this requirement can be relaxed significantly.

The electrochemical behavior of these electrodes was examined by cyclic voltammetry and by rotating disk voltammetry. The data obtained generally led to the same conclusions, so only the results of cyclic voltammetry are presented here. As might be expected, the shape of the cyclic voltammogram at the electrode array is almost completely independent of scan rate up to very high scan rates. Similarly the peak currents at these arrays do not increase with the square root of the scan rate, as expected for reversible reactions under conditions of linear diffusion. Cyclic voltammograms at the electrode arrays are compared with those at a glassy carbon disk electrode having 3 mm radius in Figure 3. As can be seen, the electrode array produces nearly a steady state current which varies little with increasing scan rate. Figure 4 displays the dependence of ln(peak current) on ln(scan rate), which for linear diffusion should be linear with a slope of 0.5. The electrode arrays exhibit neither this behavior, nor complete independence from the scan rate, indicating mixed mass transport modes.

The equation derived by Swan (16) and the much more elaborate treatment of Amatore, et al. (27) lead one to expect that these electrode arrays will be more sensitive to electron transfer rates than larger electrodes. The electron transfer rate for the oxidation of ferrocyanide on glassy carbon is known to be pH sensitive (28,29), with the reaction becoming less reversible at higher pH values. Figure 5 shows cyclic voltammograms for a customary glassy carbon electrode and a typical RVC-based array at low and neutral pH. As is readily apparent, the array shows much greater irreversibility than the glassy carbon electrode under these conditions. This behavior can be predicted qualitatively from eq. 3.

Since non-linear diffusion dominates the mass transport to the electrode

surface the current density should increase with increasing boundary density. Table II shows that current densities are 50-140% greater than those for a glassy carbon electrode with 3 mm radius under identical experimental conditions. For comparison the equivalent radius of a micro-electrode disk calculated from $P = 2/r$ is included.

Cyclic voltammetry under steady state conditions produced by non-linear diffusion produces S-shaped waves rather than the usual peaked response. A property of micro-electrodes frequently cited is that the reverse current in cyclic voltammetry approaches zero as the electrode radius decreases. The ratio of forward to reverse current should be related, therefore, to the equivalent radius calculated from the stereological data. Adams, et al. (14) have derived a relationship between the forward and reverse currents in cyclic voltammetry which can be solved for the micro-electrode radius

$$\frac{i_f}{i_r} = 1 + \frac{QD^{1/2}}{a} \left(\frac{RT}{nFv}\right)^{1/2} \tag{6}$$

where $Q = 0.92$ for micro-electrodes, a is the electrode radius, v is the scan rate, and the other symbols have their usual meaning. This equation has an intuitive justification and should apply only for cases in which $\tau \lesssim 1$ (ie, non-linear diffusion perturbs the linear diffusion profile). In the limiting case of very large radius (macro-electrode dimensions) or very fast scan rates the ratio approaches 1, the result found by Nicholson and Shain (30). Adams, et al., after deriving eq 6, did not apply it, because of the difficulty in identifying a baseline for measurement of the reverse current. Simple extrapolation of the forward scan current decay to provide a baseline for measurement of the

reverse current, the method of Nicholson and Shain, is impossible due to the steady state limiting currents.

To apply this equation we have calculated a baseline taking t = 0 at E = $E_{3/4}$ and assuming current decreases as $1/\sqrt{t}$. This calculation was first applied using data from a glassy carbon disk electrode with 3 mm radius; applying eq. 6 gave a radius of 1 mm and an intercept of 0.98, close to the expected value of 1. Table II reports the calculated radii for the five different electrode materials using this method along with the equivalent radii calculated from the stereological data. The data from which the values shown in Table II are derived are presented graphically in Figure 6. Ideally all the data, when extrapolated to infinite scan rate, should pass through i_f/i_r = 1, the limiting case for linear diffusion. Uncertainties introduced by the calculated baseline result in intercepts substantially greater than 1. For the faster scan rates of 200, 100 and 50 mV/s, where linear diffusion predominates, the current ratios are linear in $v^{-1/2}$ and yield values of a very close to those calculated from the stereological data.

At scan rates slower than 50 mV/s three of the electrode arrays show abrupt departures from linearity. Calculations show that this is very probably due to overlapping of the individual diffusion layers. Table II also lists the number of equivalent micro-disks per cm^2 and their mean equivalent spacing. Using $\sqrt{\pi D/t}$ as the rate of expansion of the diffusion layers along the electrode surface (15), the time at which the diffusion layers reach each other can be calculated (also listed in Table II). This calculation describes qualitatively the deviations seen in Figure 6. The material with the shortest interaction time

(2.9s for the 4 x 1 80) from the prediction of eq. 6 diverges at higher
scan rates and with greater abruptness than any of the other electrodes.
The two materials with the longest time to overlap, 2 x 1 45 at 13 seconds
and 4 x 1 60 at 10 seconds, show linearity through the whole range of
scan rates studied. It should be noted that in this treatment of the
data, comparing i_f/i_r, the overlap of diffusion layers not only decreases
forward currents but also increases reverse currents, because product
from one active electrode area can react at another electrode.

This treatment differs considerably from that proposed by Matsuda
(12) and recently applied by Tallman (11) because of the nature of the
arrays studied. Their calculation assumes, and their electrodes are
designed such that, the size of the spacing between the electrodes is
approximately equal to the electrode dimensions. The data published by
Matsuda indicates that diffusion layer overlap occurs in the range of
10-750 msec for his experimental conditions, using $\sqrt{\pi D/t}$ as the rate of
diffusion layer expansion along the electrode surface (15). Tallman's
case is similar in that the mean values of the micro-electrode equivalent
radius and insulating particle equivalent radius are nearly equal,
indicating diffusion layer overlap at 0.4-1.1 seconds. Their calcula-
tions are then based on a cylindrical diffusion field, the dominant mode
of mass transport on the time scale of their experiments. Because our
electrodes are separated by hundreds of microns, rather than tens of
microns, the time to overlap of diffusion layers is an order of magnitude
longer, 3-13 seconds, and hemispherical diffusion dominates mass transport
to the electrode surface during the time regime of the experiments conducted.

We conclude that the features of these electrodes are well-described
by simple theories of non-linear diffusion, and that a uniform disk

shape is not necessary for good performance of micro-electrodes. The determining factor is the boundary density of the material, and a material with a given boundary density will behave like a disk with an equivalent boundary density. This point has been made recently in another context by Myland and Oldham (31), and Saveant and co-workers (27). This has significant analytical implications, for if analytically useful results required that electrodes of this size be of a specific and controlled geometry, the possible applications would be severely restricted by the difficulty and expense of fabrication. For the chemist interested only in the analytical applications of micro-electrode technology, it is physically easier to construct electrodes using the boundary density principle than to make an array of hundreds or thousands of wires for an electrode array with the same total surface area. The electrodes studied here have the equivalent of 500 to 1500 individual fibers, a staggering number to assemble by hand. Finally, we are extending this work to many other porous electrode materials.

ACKNOWLEDGEMENT

LITERATURE CITED

(1) Clark, Jr., L. C.; Lyons, C. Ala. J. Med. Sci. 1965, 2(4), 355.

(2) Adams, R. N. Anal. Chem. 1976, 48, 1126A.

(3) Ponchon, J. L..; Cespuglio, R.; Gonon, F.; Jouvet, M.; Pujol, J. F. Anal. Chem. 1979, 51(9), 1483.

(4) Pickard, R. S. J. Neuroscience Methods 1979, 1, 301.

(5) Wightman, R. M. Anal. Chem. 1981, 53, 1125A.

(6) Siu, W.; Cobbold, R. S. C. Med. Bio. Eng. 1976, 14, 109.

(7) Aoki, K.; Osteryoung, J. J. Electroanal. Chem. 1981, 125, 315.

(8) Wightman, R. M.; Caudill, W. L.; Howell, J. O. Anal. Chem. 1982, 54, 2532.

(9) Scharifker, B.; Hills, G. J. Electroanal. Chem. 1981, 130, 81.

(10) Cushman, M. R.; Bennett, B. G.; Anderson, C. W. Anal. Chim. Acta 1981, 130, 323.

(11) Weisshaar, D. E.; Tallman, D. E. Anal. Chem. 1983, 55, 1146.

(12) Gueshi, T.; Tokuda, K.; Matsuda, H. J. Electroanal. Chem. 1978, 89, 247.

(13) Aoki, K.; Osteryoung, J. Electroanal. Chem. 1981, 122, 19.

(14) Galus, Z.; Schenk, J. O.; Adams, R. J. Electroanal. Chem. 1982, 135, 1.

(15) Reller, H.; Kirowa-Eisner, E.; Gileadi, E. J. Electroanal. Chem. 1982, 138, 65.

(16) Swan, D. Ph.D. Thesis, University of Southampton, 1979.

(17) Strohl, A. N.; Curran, D. J. Anal. Chem. 1979, 51, 353.

(18) Strohl, A. N.; Curran, D. J. Anal. Chem. 1979, 51, 1045.

(19) Strohl, A. N.; Curran, D. J. Anal. Chem. 1979, 51, 1050.

(20) Norvell, V. E.; Mamontov, G. Anal. Chem. 1977, 49, 1470.

(21) Butcher, Jr., J. A.; Chambers, J. Q.; Pagni, R. M. J. Am. Chem. Soc. 1978, 100, 1012.

(22) Schreiner, M.; O'Dea, J. J.; Sleszynski, N.; Osteryoung, J. Submitted to Anal. Chem.

(23) Underwood, E. E. Quantitative Stereology, Addison-Wesley Publishing Co. 1970.

(24) Weibel, E. R. Stereological Methods, Vol. 1, Practical Methods for Biological Morphometry, Academic Press, 1979.

(25) Cochran, W. C. Sampling Techniques, p. 124, Wiley and Sons, N.Y. 1953.

(26) Kline, S. J.; McClintock, F. A. Mech. Eng. 1953, 3.

(27) Amatore, C.; Saveant, J. M.; Tessier, D. J. Electroanal. Chem. 1983, 147, 39-51.

(28) Blaedel, W. J.; Schieffer, G. W. J. Electroanal. Chem. 1977, 80, 259.

(29) Albertson, D. E.; Blount, H. N.; Hawkridge, F. M. Anal. Chem. 1979, 51, 556.

(30) Nicholson, R. S.; Shain, I. Anal. Chem. 1964, 36, 706.

(31) Myland, Jan C.; Oldham, Keith B. J. Electroanal. Chem. 1983, 147, 295-300.

Figure Captions

Figure 1:. Configuration of electrode constructed from RVC infused with non-conductive epoxy; a) electrode shaft, b) contact screw, c) rubber "O" ring, d) non-conductive epoxy sheath, e) contact nut, f) silver epoxy in RVC, g) RVC infused with non-conductive epoxy.

Figure 2: Micrographs of two different electrodes representative of the general class of RVC based materials. A) 2 x 1 100 electrode magnified 50X, B) the same electrode with the central section magnified to 100X. The structure pictured is approximately 1000 microns long and 30 microns wide, C) 4 x 1 80 electrode magnified 50X, D) the central section of the same electrode magnified 100X. The main structure pictured is 700 microns long and from 30 to 120 microns wide.

Figure 3: A cyclic voltammogram of 5 mM $Fe(CN)_6^{-4}$ in 1 M KCl, pH = 2.7 a) 2 x 1 100 electrode array at 100 mV/s, b) same electrode at 500 mV/s, c) 6 mm GCE at 100 mV/s, d) the same electrode at 500 mV/s.

Figure 4: The dependence of the cyclic voltammogram peak current on the scan rate for a 6 mm GCE and five different RVC-based electrode arrays; a) GCE, b) 4 x 1 80, c) 4 x 1 100, d) 4 x 1 60, e) 2 x 1 100, f) 2 x 1 45.

Figure 5: Voltammograms of 5 mM $Fe(CN)_6^{-4}$ at pH 2.7 (a and c) and pH 7.7 (b and d) for a 4 x 1 80 micro-electrode array (a and b) and a 6 mm GCE (c and d).

Figure 6: The ratio of the forward to reverse current, using a calculated $1/\sqrt{t}$ decay for baseline subtraction, versus $1/\sqrt{v}$ (the scan rate in V/s) for a GCE and five different electrode arrays; a) 2 x 1 45, b) 4 x 1 60, c) 6mm GCE, d) 2 x 1 100, e) 4 x 1 100, f) 4 x 1 80.

CREDIT

Table I. Stereological description of electrodes fabricated from RVC.

Specimen Markings	Section Area mm² A	Carbon Area Fraction mm²/mm² A_s	95% C.L.	Carbon Surface Area, mm²	Carbon Boundary Length per Section Area mm/mm² L_s	95% C.L.	Carbon Boundary Length, mm	Carbon Boundary Density mm/mm L_s/A_s	Uncertainty
2x1,45#1	101	0.043	0.007	4.3	1.69	0.12	171	39	7
2x1,45#2	101	0.044	0.006	4.5	1.71	0.17	173	39	7
2x1,45#3	102	0.056	0.008	5.7	1.55	0.18	158	28	5
4x1,60#1	102	0.067	0.008	6.8	2.30	0.10	235	34	4
4x1,60#2	102	0.060	0.008	6.1	2.36	0.16	241	40	6
4x1,60#3	103	0.074	0.012	7.6	2.40	0.15	247	33	6
4x1,80#1	102	0.101	0.008	10.3	4.08	0.21	416	40	4
4x1,80#2	102	0.110	0.008	11.3	4.16	0.22	424	38	4
4x1,80#3	104	0.103	0.009	10.6	4.03	0.22	419	39	4
2x1,100#1	104	0.056	0.008	5.8	3.22	0.21	335	57	4
2x1,100#2	99	0.052	0.005	5.1	3.18	0.15	315	61	8
4x1,100#1	102	0.083	0.008	8.5	3.54	0.22	361	43	5
4x1,100#2	102	0.074	0.008	7.6	3.40	0.12	347	46	5

Table II. Current densities and calculated equivalent radii.

Sample type	Current densities, μA/mM cm²[a]	Equivalent radius,[a] $a=2/P$, μm	Equivalent radius, voltammetry,[c] μm	Number of equivalent[d] electrodes per cm	Equivalent distance between electrodes, μm	Time to diffusion layer overlap
Glassy carbon disk, r=3mm	78	3,000[b]	950			
2 x 1 45	117	51	51	529	435	13 seconds
2 x 1 100	188	34	34	1453	263	4.4 seconds
4 x 1 60	145	56	60	599	408	9.8 seconds
4 x 1 80	152	51	45	1653	246	2.9 seconds
4 x 1 100	177	45	40	1544	254	3.6 seconds

a) $P = L_a/A_a$ from Table I

b) geometric radius
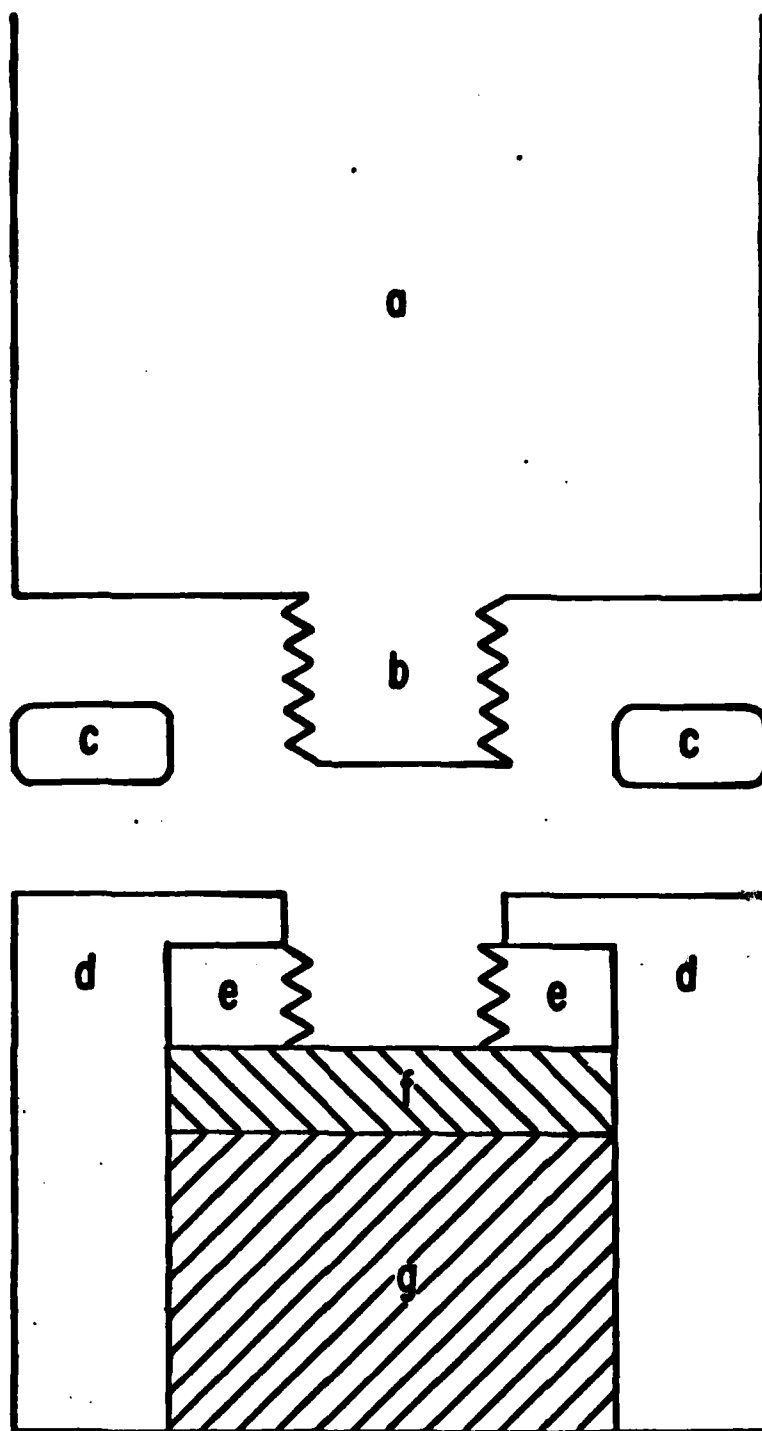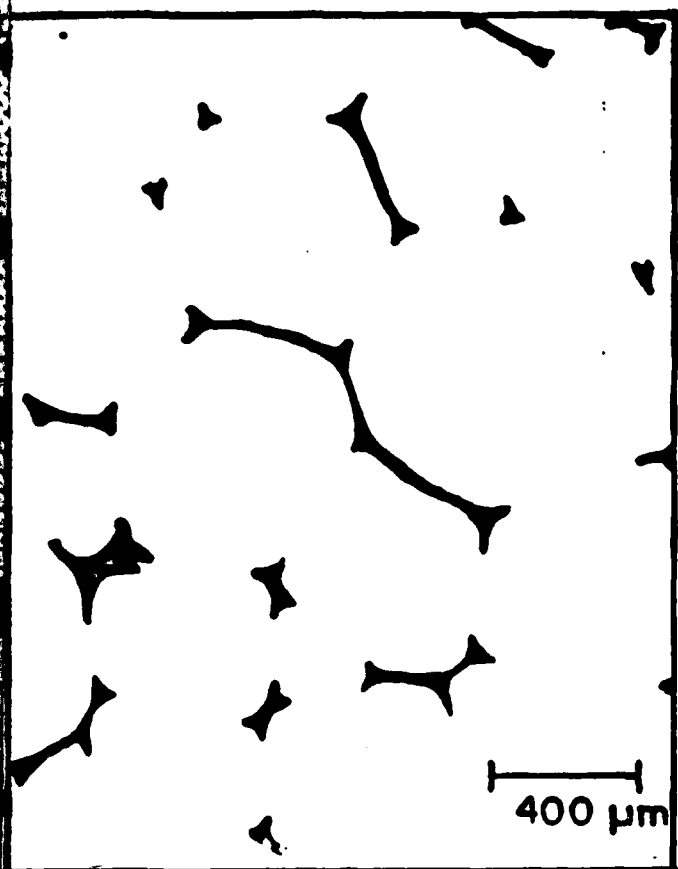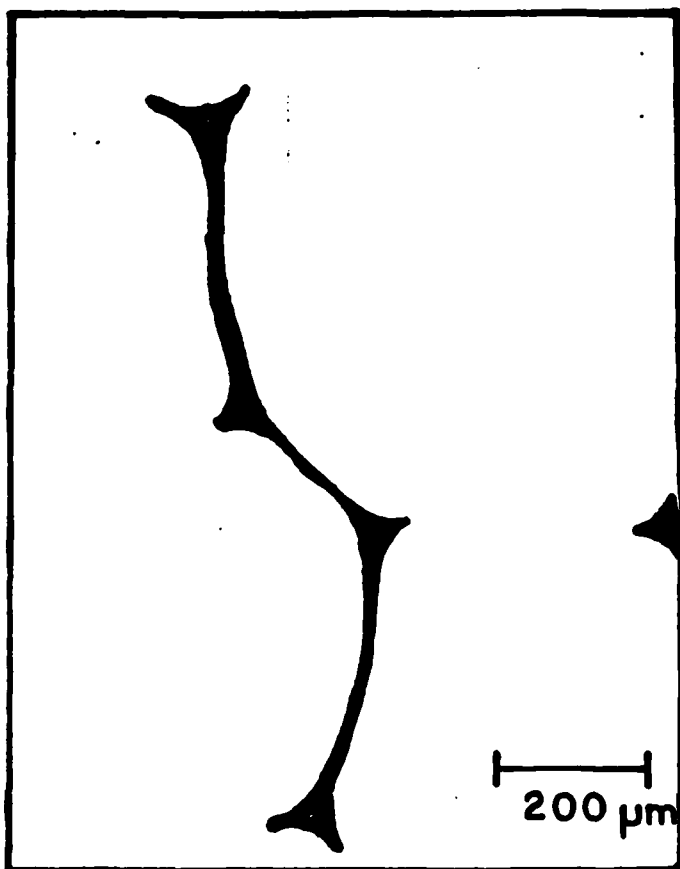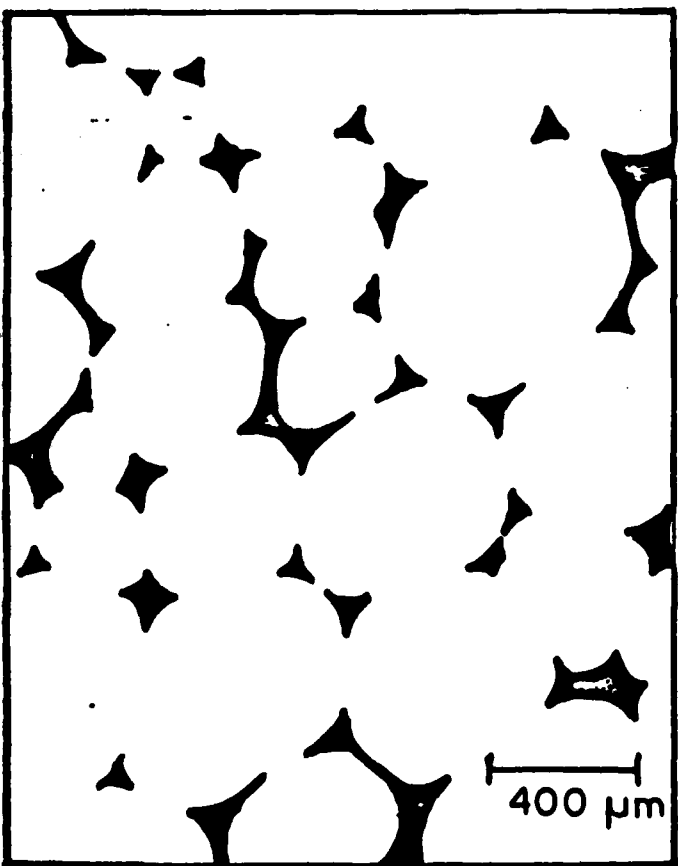
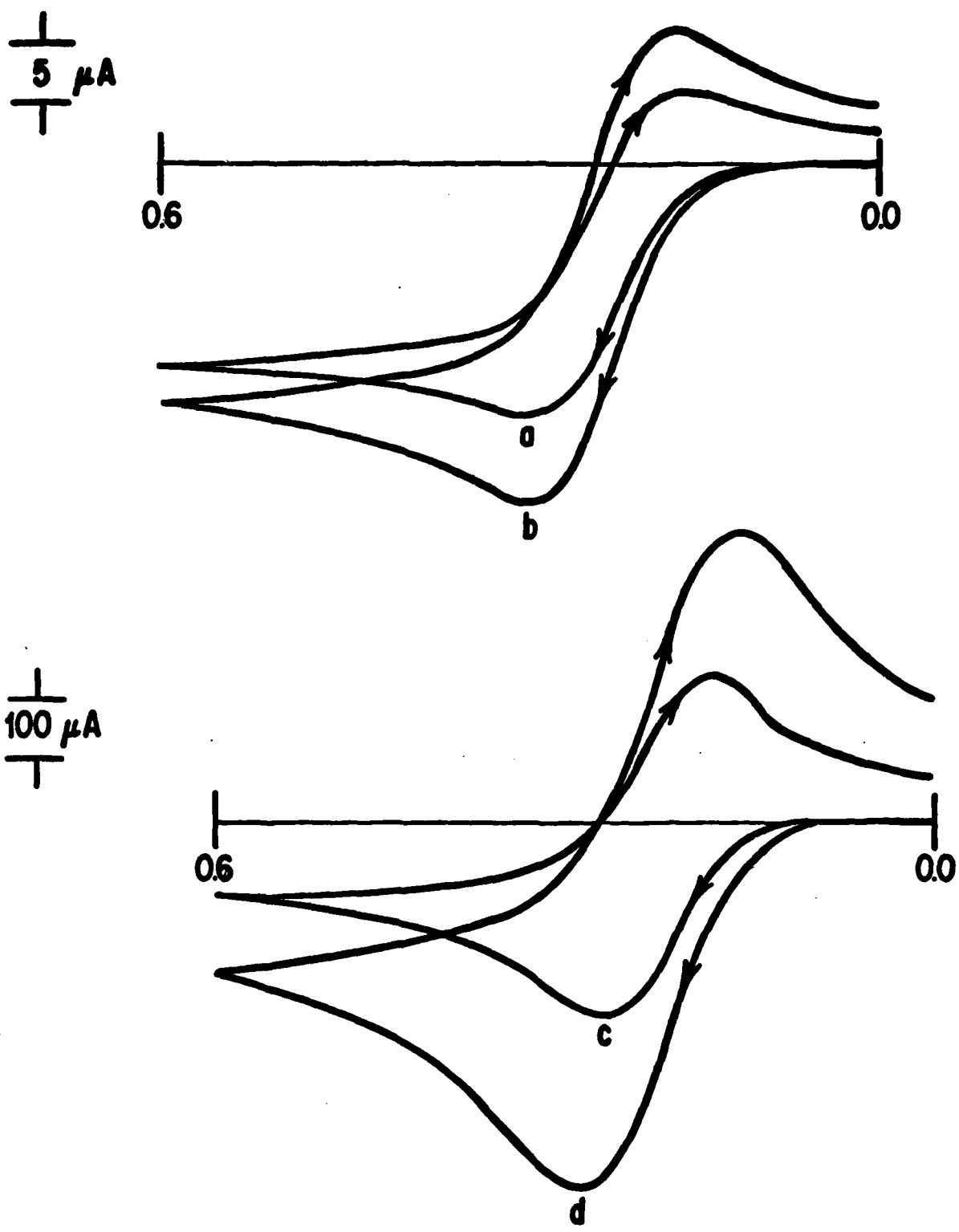c) Data of Fig. 6 analyzed according to eq 10

d) $A_a/\pi a^2$
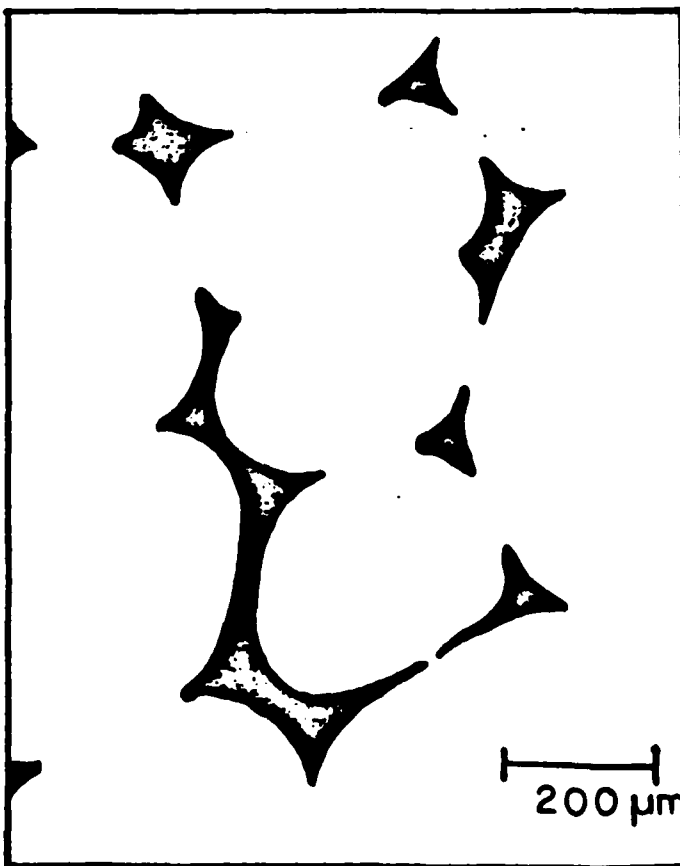
FIGURE 1
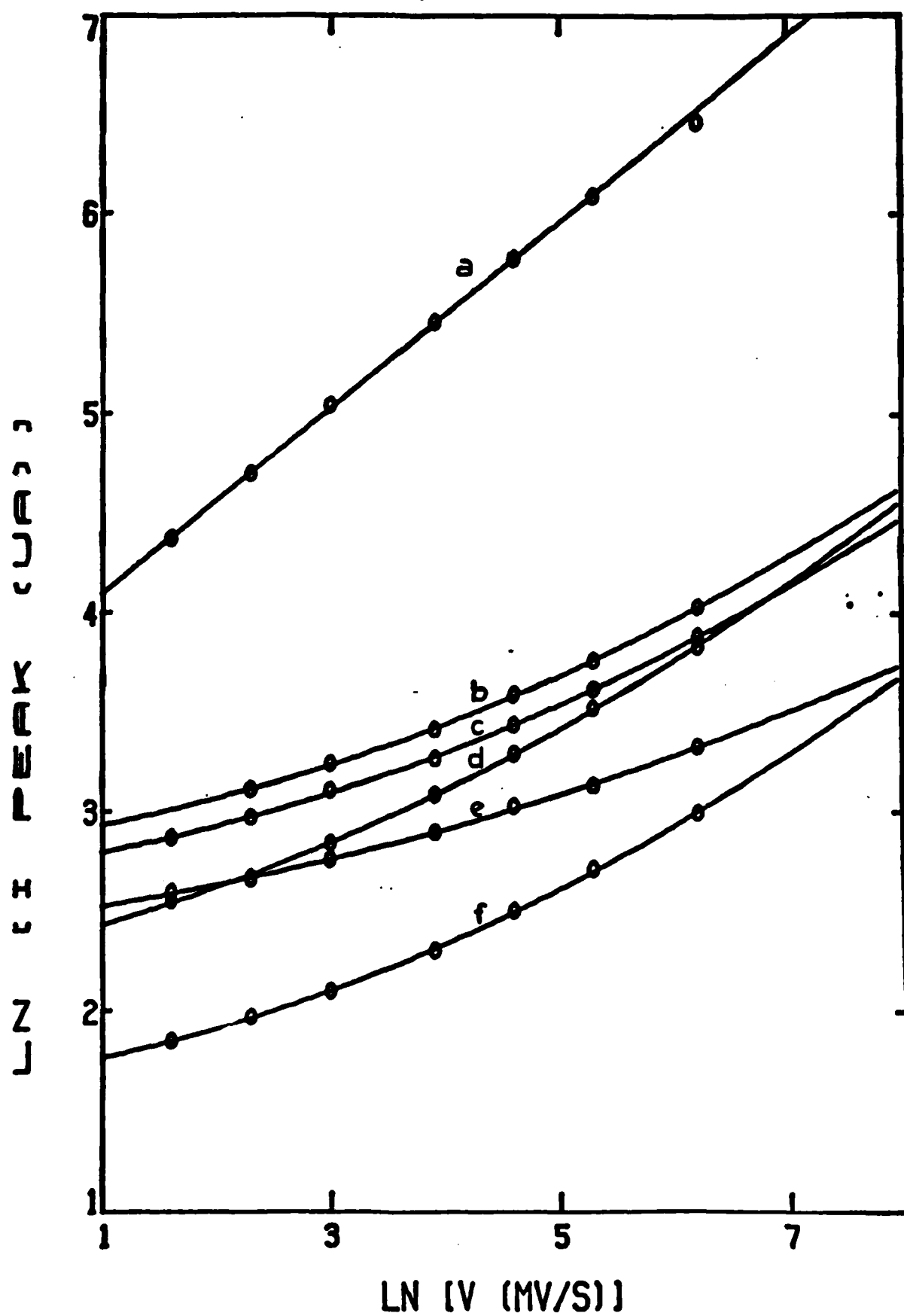
FIGURE 2

FIGURE 3

FIGURE 4

FIGURE 5

FIGURE 6

SP472-3/A1
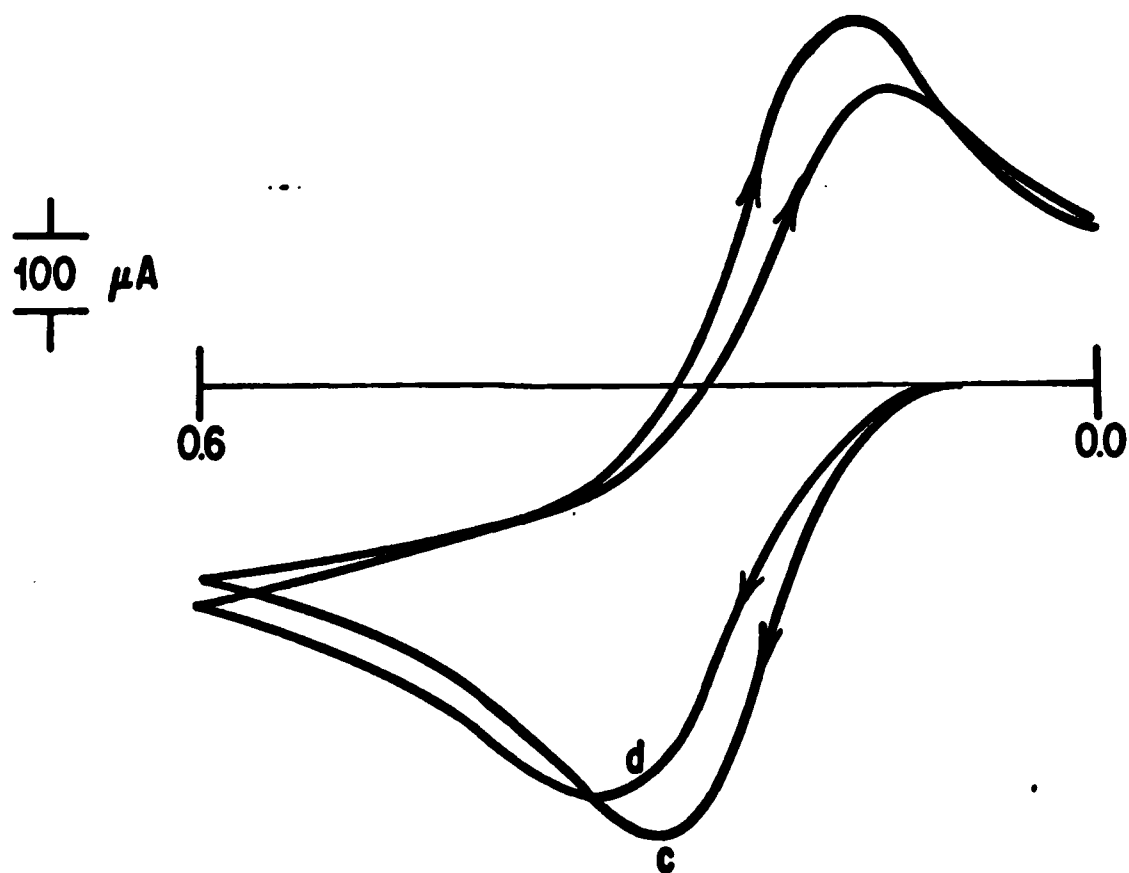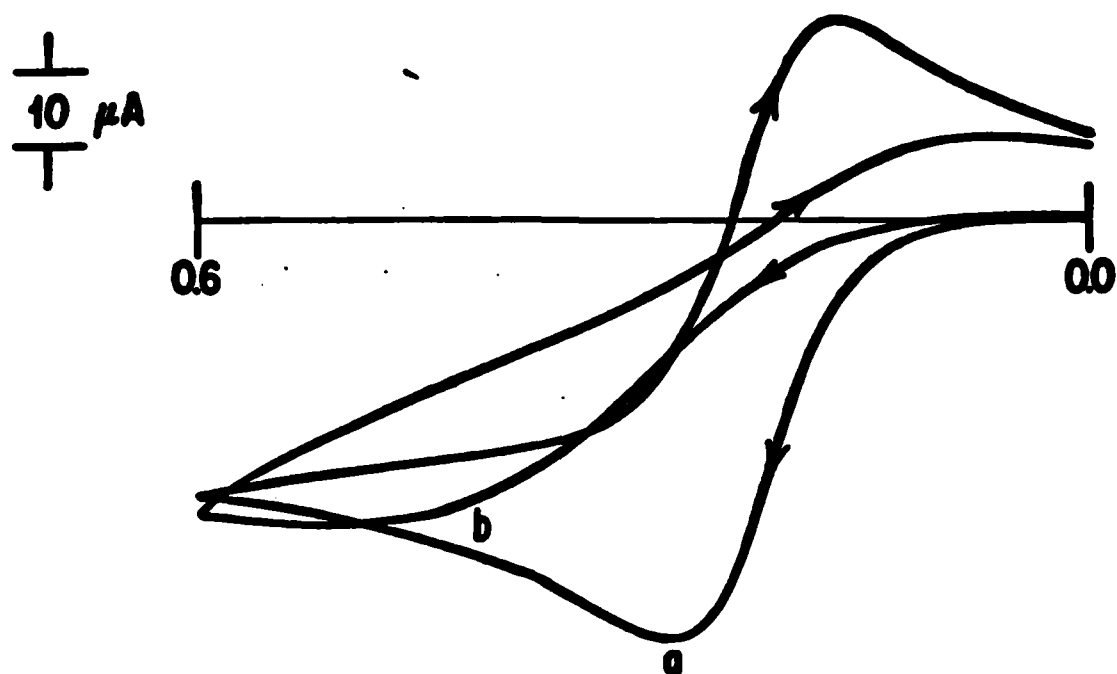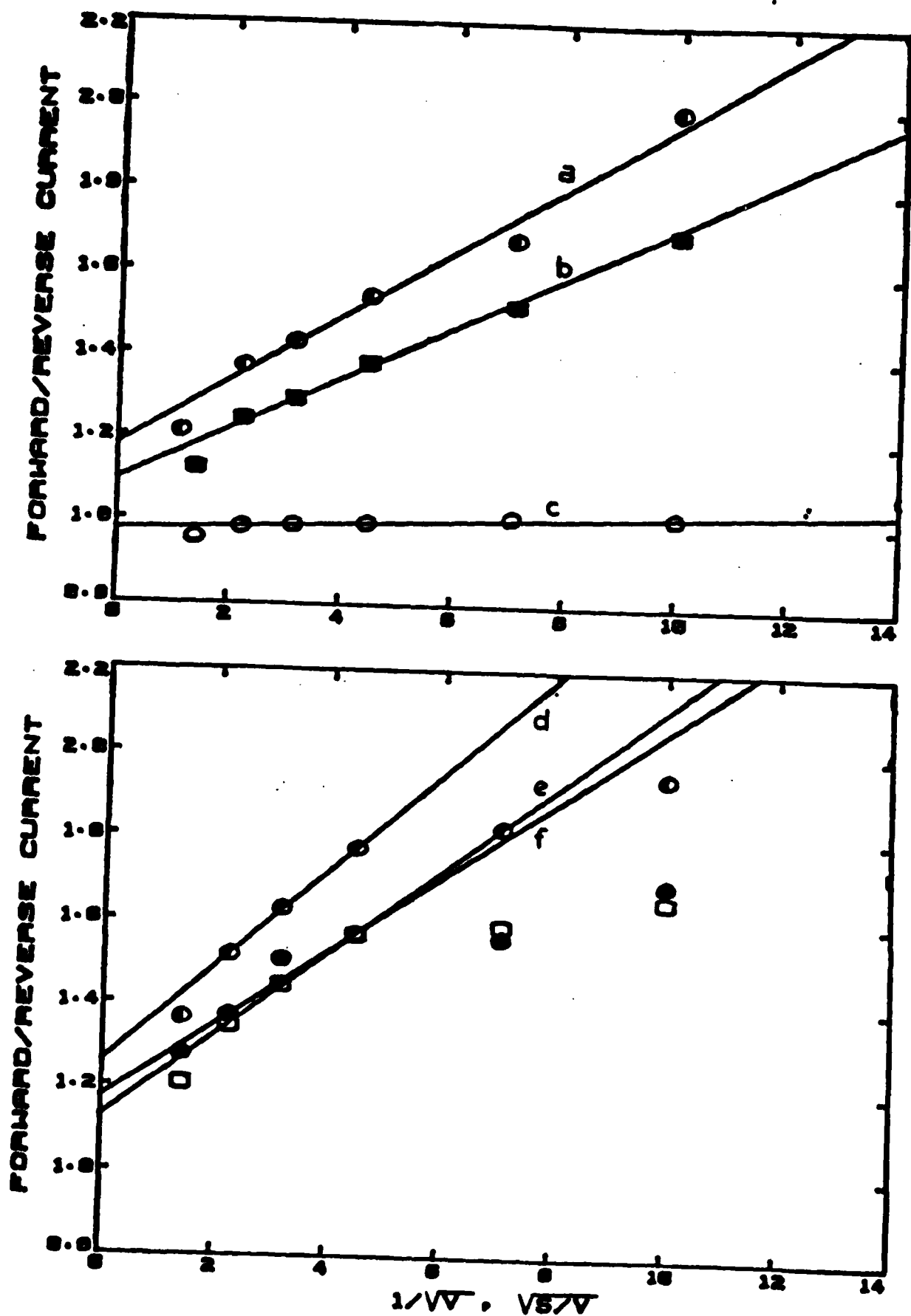
TECHNICAL REPORT DISTRIBUTION LIST, GEN

	No. Copies		No. Copies
Office of Naval Research Attn: Code 472 800 North Quincy Street Arlington, Virginia 22217	2	U.S. Army Research Office Attn: CRD-AA-IP P.O. Box 1211 Research Triangle Park, N.C. 27709	1
ONR Western Regional Office Attn: Dr. R. J. Marcus 1030 East Green Street Pasadena, California 91106	1	Naval Ocean Systems Center Attn: Mr. Joe McCartney San Diego, California 92152	1
ONR Eastern Regional Office Attn: Dr. L. H. Peebles Building 114, Section D 666 Summer Street Boston, Massachusetts 02210	1	Naval Weapons Center Attn: Dr. A. B. Amster, Chemistry Division China Lake, California 93555	1
Director, Naval Research Laboratory Attn: Code 6100 Washington, D.C. 20390	1	Naval Civil Engineering Laboratory Attn: Dr. R. W. Drisko Port Hueneme, California 93401	1
The Assistant Secretary of the Navy (RE&S) Department of the Navy Room 4E736, Pentagon Washington, D.C. 20350	1	Department of Physics & Chemistry Naval Postgraduate School Monterey, California 93940	1
Commander, Naval Air Systems Command Attn: Code 310C (H. Rosenwasser) Department of the Navy Washington, D.C. 20360	1	Scientific Advisor Commandant of the Marine Corps (Code RD-1) Washington, D.C. 20380	1
Defense Technical Information Center Building 5, Cameron Station Alexandria, Virginia 22314	12	Naval Ship Research and Development Center Attn: Dr. G. Bosmajian, Applied Chemistry Division Annapolis, Maryland 21401	1
Dr. Fred Saalfeld Chemistry Division, Code 6100 Naval Research Laboratory Washington, D.C. 20375	1	Naval Ocean Systems Center Attn: Dr. S. Yamamoto, Marine Sciences Division San Diego, California 91232	1
		Mr. John Boyle Materials Branch Naval Ship Engineering Center Philadelphia, Pennsylvania 19112	1

SP472-3/A11

472:GAN:716:ddc
78u472-608

TECHNICAL REPORT DISTRIBUTION LIST, 359

	No. Copies		No. Copies
Dr. Paul Delahay Department of Chemistry New York University New York, New York 10003	1	Dr. P. J. Hendra Department of Chemistry University of Southhampton Southhampton SO9 5NH United Kingdom	1
Dr. E. Yeager Department of Chemistry Case Western Reserve University Cleveland, Ohio 41106	1	Dr. Sam Perone Department of Chemistry Purdue University West Lafayette, Indiana 47907	1
Dr. D. N. Bennion Department of Chemical Engineering Brigham Young University Provo, Utah 84602	1	Dr. Royce W. Murray Department of Chemistry University of North Carolina Chapel Hill, North Carolina 27514	1
Dr. R. A. Marcus Department of Chemistry California Institute of Technology Pasadena, California 91125	1	Naval Ocean Systems Center Attn: Technical Library San Diego, California 92152	1
Dr. J. J. Auborn Bell Laboratories Murray Hill, New Jersey 07974	1	Dr. C. E. Mueller The Electrochemistry Branch Materials Division, Research & Technology Department Naval Surface Weapons Center	
Dr. Adam Heller Bell Laboratories Murray Hill, New Jersey 07974	1	White Oak Laboratory Silver Spring, Maryland 20910	1
Dr. T. Katan Lockheed Missiles & Space Co, Inc. P.O. Box 504 Sunnyvale, California 94088	1	Dr. G. Goodman Globe-Union Incorporated 5757 North Green Bay Avenue Milwaukee, Wisconsin 53201	1
Dr. Joseph Singer, Code 302-1 NASA-Lewis 21000 Brookpark Road Cleveland, Ohio 44135	1	Dr. J. Boechler Electrochimica Corporation Attention: Technical Library 2485 Charleston Road Mountain View, California 94040	1
Dr. B. Brummer EIC Incorporated 55 Chapel Street Newton, Massachusetts 02158	1	Dr. P. P. Schmidt Department of Chemistry Oakland University Rochester, Michigan 48063	1
Library P. R. Mallory and Company, Inc. Northwest Industrial Park Burlington, Massachusetts 01803	1	Dr. H. Richtol Chemistry Department Rensselaer Polytechnic Institute Troy, New York 12181	1

SP472-3/B13

TECHNICAL REPORT DISTRIBUTION LIST, 359

	No. Copies		No. Copies
Dr. A. B. Ellis Chemistry Department University of Wisconsin Madison, Wisconsin 53706	1	Dr. R. P. Van Duyne Department of Chemistry Northwestern University Evanston, Illinois 60201	1
Dr. M. Wrighton Chemistry Department Massachusetts Institute of Technology Cambridge, Massachusetts 02139	1	Dr. B. Stanley Pons Department of Chemistry University of Alberta Edmonton, Alberta CANADA T6G 2G2	1
Larry E. Plew Naval Weapons Support Center Code 30736, Building 2906 Crane, Indiana 47522	1	Dr. Michael J. Weaver Department of Chemistry Michigan State University East Lansing, Michigan 48824	1
S. Ruby DOE (STOR) 600 E Street Washington, D.C. 20545	1	Dr. R. David Rauh EIC Corporation 55 Chapel Street Newton, Massachusetts 02158	1
Dr. Aaron Wold Brown University Department of Chemistry Providence, Rhode Island 02192	1	Dr. J. David Margerum Research Laboratories Division Hughes Aircraft Company 3011 Malibu Canyon Road Malibu, California 90265	1
Dr. R. C. Chudacek McGraw-Edison Company Edison Battery Division Post Office Box 28 Bloomfield, New Jersey 07003	1	Dr. Martin Fleischmann Department of Chemistry University of Southampton Southampton SO9 5NH England	1
Dr. A. J. Bard University of Texas Department of Chemistry Austin, Texas 78712	1	Dr. Janet Osteryoung Department of Chemistry State University of New York at Buffalo Buffalo, New York 14214	1
Dr. M. M. Nicholson Electronics Research Center Rockwell International 3370 Miraloma Avenue Anaheim, California	1	Dr. R. A. Osteryoung Department of Chemistry State University of New York at Buffalo Buffalo, New York 14214	1
Dr. Donald W. Ernst Naval Surface Weapons Center Code R-33 White Oak Laboratory Silver Spring, Maryland 20910	1	Mr. James R. Moden Naval Underwater Systems Center Code 3632 Newport, Rhode Island 02840	1

TECHNICAL REPORT DISTRIBUTION LIST, 359

	No. Copies		No. Copies
Dr. R. Nowak Naval Research Laboratory Code 6130 Washington, D.C. 20375	1	Dr. Bernard Spielvogel U.S. Army Research Office P.O. Box 12211 Research Triangle Park, NC 27709	1
Dr. John P. Houlihan Shenango Valley Campus Pennsylvania State University Sharon, Pennsylvania 16146	1	Dr. Denton Elliott Air Force Office of Scientific Research Bolling AFB Washington, DC 20332	1
Dr. D. F. Shriver Department of Chemistry Northwestern University Evanston, Illinois 60201	1	Dr. David Aikens Chemistry Department Rensselaer Polytechnic Institute Troy, NY 12181	1
Dr. D. N. Whitmore Department of Materials Science Northwestern University Evanston, Illinois 60201	1	Dr. A. P. B. Lever Chemistry Department York University Downsview, Ontario M3J1P3 Canada	1
Dr. Alan Bewick Department of Chemistry The University Southampton, SO9 5NH England	1	Mr. Maurice F. Murphy Naval Sea Systems Command 63R32 2221 Jefferson Davis Highway Arlington, VA 20360	1
Dr. A. Nimy NAVSEA-5433 NC #4 2541 Jefferson Davis Highway Arlington, Virginia 20362	1	Dr. Stanislaw Szpak Naval Ocean Systems Center Code 6343 San Diego, CA 95152	1
Dr. John Kincaid Department of the Navy Stategic System Project Office Room 901 Washington, DC 20376	1	Dr. Gregory Farrington Department of Materials Science & Engineering University of Pennsylvania Philadelphia, PA 19104	1
M. L. Robertson Manager, Electrochemical Power Sonices Division Naval Weapons Support Center Crane, Indiana 47522	1	Dr. Bruce Dunn Department of Engineering & Applied Science University of California Los Angeles, CA 90024	1
Dr. Elton Cairns Energy & Environment Division Lawrence Berkeley Laboratory University of California Berkeley, California 94720	1		

TECHNICAL REPORT DISTRIBUTION LIST, 359

No.
Copies

Dr. Micha Tomkiewicz
Department of Physics
Brooklyn College
Brooklyn, NY 11210   1

Dr. Lesser Blum
Department of Physics
University of Puerto Rico
Rio Piedras, PR 00931   1

Dr. Joseph Gordon II
IBM Corporation
K33/281
5600 Cottle Road
San Jose, CA 95193   1

Dr. Robert Somoano
Jet Propulsion Laboratory
California Institute of Technology
Pasadena, CA 91103   1

END

FILMED

11-83

DTIC